

# Direct detection rates for Kaluza-Klein dark matter

Debasish Majumdar\*

*Theory Division, Saha Institute of Nuclear Physics, 1/AF Bidhannagar, Kolkata 700064, India*

(Received 12 December 2002; published 19 May 2003)

We consider the lightest Kaluza-Klein particles at the  $N=1$  mode (LKP) of universal extra dimensions to be a candidate for cold dark matter. We discuss the possibility of detecting them through direct detection at earth bound detectors. The detection rates for such particles are predicted for germanium, NaI, and xenon detectors. We have also calculated the nature of annual modulation for the dark matter signals in these detectors for the case of LKP dark matter. The variation of detection rates with the variation of rotational speed of the Solar System in the galactic rest frame is also addressed.

DOI: 10.1103/PhysRevD.67.095010

PACS number(s): 12.60.-i, 11.10.Kk, 95.35.+d

## I. INTRODUCTION

There is strong indirect evidence (gravitational) from various observations such as velocity curves of spiral galaxies, gravitational lensing, etc., in favor of the existence of an enormous amount of invisible, nonluminous matter or dark matter in the Universe. This dark matter constitutes more than 90% of the matter in the Universe. Although the constituents of dark matter still remain a mystery, the indirect evidence suggests that a large part of dark matter should be nonbaryonic in nature. They are stable, heavy, nonrelativistic [cold dark matter (CDM)] and are weakly interacting. Therefore they are often known as weakly interacting massive particles (WIMPs).

Currently the most popular candidate for CDM is the lightest supersymmetric particle (LSP) which of course is not a standard model particle. In the minimal supersymmetric standard model (MSSM), the LSP is a neutralino ( $\chi$ ). A neutralino is a Majorana fermion and it is a superposition of supersymmetric partners of neutral U(1) and SU(2) gauge bosons and neutral Higgs bosons. The conservation of  $R$  parity ensures that the LSP is a stable particle. In the literature there is a lot of work in which the neutralino in the MSSM and supergravity models is considered as a dark matter candidate [1–5]. In a recent work the neutralino LSP as a dark matter candidate from the minimal anomaly mediated supersymmetry breaking (MAMSB) model has been addressed [6].

In the present work we consider a bosonic particle, unlike the fermionic supersymmetric (SUSY) particle, to be a candidate for dark matter. This particle is a lightest Kaluza-Klein (KK) particle (LKP) in universal extra dimension (UED) [7,8]. The Kaluza-Klein theory [9] is a five-dimensional theory with four space-time dimensions and one extra space dimension, the extra dimension (fifth dimension) is assumed to be compact. The fifth dimension has the topology of a circle with the compactification radius of the order of Planck scale. The topology of this five-dimensional space-time is  $R^4 \times S^1$  and the fifth coordinate  $y$  is periodic with  $0 \leq y/R \leq 2\pi$ ,  $R$  being the radius of the circle. When the wave equation is solved in this space-time, this periodic boundary

condition leads to integer eigenvalues for the momentum and consequently one obtains an infinite tower of mass  $m_n$  with  $m_n^2 = n^2/R^2$ . This tower is known as a Kaluza-Klein tower. The universal extra dimension (UED) model is one in which all standard model (SM) particles can propagate in compact extra dimensions. In UED therefore every standard model particle has a KK partner in the KK tower. In the resulting theory only an even number or odd number of KK modes interact. This parity conservation of KK particles ensures that the lightest KK particle or LKP is stable and cannot decay into SM zero modes. Thus LKP can be a candidate for cold dark matter. Following [7] in the present calculation, the first KK partner  $B^1$  of hypercharge gauge boson is the LKP. The LKP is a bosonic particle whereas LSP is a fermionic particle.

The direct detection of WIMP dark matter by a terrestrial detector uses the principle of elastic scattering of WIMP off detector nuclei. But this is a difficult task as the WIMP-nucleus interaction is very feeble. The energy deposited by a WIMP of mass a few GeV to 1 TeV on a detector nucleus is not more than 100 keV. Hence for direct detection of WIMP the detector has to be of low energy threshold and of low background.

For this calculation of direct detection rates using the phenomenon of elastic scattering, it is required to estimate the mass range for LKP dark matter. The collider bound for universal extra dimension gives  $1/R \geq 300$  GeV [10] and thus mass  $m_{B^1}$  of  $B^1$  should not be below 300 GeV. Again the chosen mass for LKP should be consistent with the relic density for KK particles. In a recent calculation, Servant *et al.* [11] has found the range for  $m_{B^1}$  between 600 and 1200 GeV as being consistent with the dark matter content of the universe. In the present calculation, we consider the values of  $m_{B^1}$  in the range between 600 and 1200 GeV.

There are certain ongoing experiments and proposed experiments for WIMP direct search. The target materials generally used are NaI, Ge, Si, Xe, etc. NaI (100 kg) is used for the DAMA experiment and the near future LIBRA (large sodium iodine bulk for rare processes) experiment (250 kg of NaI) [12]. These setups are at Gran Sasso tunnel in Italy. The DAMA Collaboration claimed to have detected this annual modulation of WIMP through their direct WIMP detection experiments. Their analysis suggests the possible presence of dark matter with a mass around 50 GeV. This result is certainly far below the range of LKP mass discussed above. The

\*Email address: debasish@theory.saha.ernet.in

cryogenic dark matter search (CDMS) detector employs low temperature Ge and Si as detector materials to detect WIMPs via their elastic scattering off these nuclei [13]. This is housed in a 10.6 m tunnel ( $\sim 16$  m.w.e) at Stanford Underground Facility beneath the University of Stanford. Although their direct search results are compatible with some regions of  $3\text{-}\sigma$  allowed regions for DAMA analysis, it excludes DAMA results if standard WIMP interaction and a standard dark matter halo is assumed. The EDELWEISS dark matter search experiment which also uses a cryogenic Ge detector at Frejus tunnel, 4800 m.w.e under the French-Italian Alps observed no nuclear recoils in the fiducial volume [14]. This experiment excludes DAMA results at more than 99.8% C.L. The lower bound of recoil energy in this experiment was 20 keV. The Heidelberg dark matter search (HDMS) uses in their inner detector, highly pure  $^{73}\text{Ge}$  crystals [15] and with a very low energy threshold. They have recently made available their 26.5 kg day analysis. The recent low threshold experiment GENIUS (Germanium in liquid Nitrogen Underground Setup) [16] at Gran Sasso tunnel in Italy has started its operation. Although a project for  $\beta\beta$ -decay search, due to its very low threshold (and expected to be reduced further), GENIUS is a potential detector for WIMP direct detection experiments and for detection of low energy solar neutrinos like  $pp$ -neutrinos or  $^7\text{Be}$  neutrinos. In the GENIUS experiment highly pure  $^{76}\text{Ge}$  is used as detector material. For dark matter search, 100 kg of the detector material is suspended in a tank of liquid nitrogen. The threshold for germanium detectors is around 11 keV. But for GENIUS, this threshold will be reduced to 500 eV in the future. This will be increased in the future. The proposed XENON detector [17] will consist of 1000 kg of  $^{131}\text{Xe}$  with 4 keV threshold.

In this work we calculate the direct detection rates for three target materials considering the LKP to be the cold dark matter candidate. These materials are  $^{76}\text{Ge}$ , NaI, and  $^{131}\text{Xe}$ .

The theoretical predictions of event rates have been addressed by several authors [18–21]. In Ref. [18] Gaisser *et al.* gave a theoretical overview of the event rate prediction. In Ref. [19] direct detection rates for detectors with various detecting material is given. In Refs. [20,21], the emphasis was mainly to analyze DAMA/NaI data. A recent calculation of detection rates for KK dark matter is given in Ref. [22].

The paper is organized as follows. In Sec. II we give the theory for calculation of detection rates for three types of detector materials namely  $^{76}\text{Ge}$ , NaI, and xenon ( $^{131}\text{Xe}$ ). The actual calculation of differential rates for various choices of LKP mass and other parameters is discussed in Sec. III. In Sec. IV we give some concluding remarks.

## II. THEORY

Differential detection rate of WIMPs per unit detector mass can be written as

$$\frac{dR}{d|\mathbf{q}|^2} = N_T \int \Phi \frac{d\sigma}{d|\mathbf{q}|^2} f(v) dv, \quad (1)$$

where  $N_T$  denotes the number of target nuclei per unit mass of the detector,  $\Phi$  being the WIMP flux,  $v$  is WIMP velocity in the reference frame of Earth, and  $f(v)$  is the distribution of this velocity. The integration is over all possible kinematic configurations in the scattering process. In the above,  $|\mathbf{q}|$  is the momentum transferred to the nucleus in WIMP-nucleus scattering. Nuclear recoil energy  $E_R$  is

$$E_R = |\mathbf{q}|^2 / 2m_{\text{nuc}} = m_{\text{red}}^2 v^2 (1 - \cos \theta) / m_{\text{nuc}}, \quad (2)$$

$$m_{\text{red}} = \frac{m_{B^1} m_{\text{nuc}}}{m_{B^1} + m_{\text{nuc}}}, \quad (3)$$

where  $\theta$  is the scattering angle in WIMP-nucleus center of momentum frame,  $m_{\text{nuc}}$  is the nuclear mass, and  $m_{B^1}$  is the WIMP mass.

Now expressing  $\Phi$  in terms of local WIMP density  $\rho_\chi$ , WIMP velocity  $v$ , and WIMP mass  $m_{B^1}$  and writing  $|\mathbf{q}|^2$  in terms of nuclear recoil energy  $E_R$  with noting that  $N_T = 1/m_{\text{nuc}}$ , Eq. (1) takes the form

$$\frac{dR}{dE_R} = \frac{\rho_\chi}{m_{B^1}} 2 \frac{d\sigma}{d|\mathbf{q}|^2} \int_{v_{\min}}^\infty v f(v) dv, \quad (4)$$

$$v_{\min} = \left[ \frac{m_{\text{nuc}} E_R}{2m_{\text{red}}^2} \right]^{1/2}.$$

The WIMP-nucleus (or WIMP-nucleon) scattering cross section has two parts, namely the spin-independent or scalar cross section and the spin-dependent cross section. Here we make the assumption that the scalar cross section dominates over the spin-dependent cross section.<sup>1</sup> Following Ref. [23] the WIMP-nucleus differential cross section for the scalar interaction can be written as

$$\frac{d\sigma}{d|\mathbf{q}|^2} = \frac{\sigma_{\text{scalar}}}{4m_{\text{red}}^2 v^2} F^2(E_R). \quad (5)$$

In the above  $\sigma_{\text{scalar}}$  is the WIMP-nucleus scalar cross section and  $F(E_R)$  is the nuclear form factor given by [24,25]

$$F(E_R) = \left[ \frac{3j_1(qR_1)}{qR_1} \right] \exp\left(-\frac{q^2 s^2}{2}\right), \quad (6)$$

$$R_1 = (r^2 - 5s^2)^{1/2},$$

$$r = 1.2A^{1/3},$$

where the thickness parameter of the nuclear surface is given by  $s \simeq 1$  fm,  $A$  is the mass number of the nucleus, and  $j_1(qR_1)$  is the spherical Bessel function of index 1.

<sup>1</sup>For bosonic KK dark matter scalar cross-section effects dominate [7].

For the distribution  $f(v_{\text{gal}})$  of WIMP velocity  $v_{\text{gal}}$  with respect to the galactic rest frame, a Maxwellian form is considered here. The velocity  $v$  [and  $f(v)$ ] with respect to the Earth rest frame can then be obtained by making the transformation

$$\mathbf{v} = \mathbf{v}_{\text{gal}} - \mathbf{v}_{\oplus}, \quad (7)$$

where  $v_{\oplus}$  is the velocity of Earth with respect to the galactic rest frame and is given by

$$v_{\oplus} = v_{\odot} + v_{\text{orb}} \cos \gamma \cos \left( \frac{2\pi(t-t_0)}{T} \right). \quad (8)$$

In Eq. (8),  $T=1$  year is the time period of the Earth's motion around the Sun,  $t_0 \equiv \text{June } 2$ ,  $v_{\text{orb}}$  is Earth's orbital speed, and  $\gamma \approx 60^\circ$  is the angle subtended by Earth's orbital plane at the galactic plane. The speed of solar system  $v_{\odot}$  in the galactic rest frame is given by

$$v_{\odot} = v_0 + v_{\text{pec}}, \quad (9)$$

where  $v_0$  is the circular velocity of the local system at the position of solar system and  $v_{\text{pec}}$  is the speed of solar system with respect to the local system. The latter is also called peculiar velocity and its value is 12 km/s. Although the physical range of  $v_0$  is given by [26,27]  $170 \text{ km/s} \leq v_0 \leq 270 \text{ km/s}$  (90% C.L.), in the present work we consider the central value of  $v_0 = 220 \text{ km/s}$ . Here we mention that Eq. (8) is the origin of annual modulation of the WIMP signal.

Defining a dimensionless quantity  $T(E_R)$  as

$$T(E_R) = \frac{\sqrt{\pi}}{2} v_0 \int_{v_{\min}}^{\infty} \frac{f(v)}{v} dv \quad (10)$$

and noting that  $T(E_R)$  can be expressed as [23]

$$T(E_R) = \frac{\sqrt{\pi}}{4v_{\oplus}} v_0 \left[ \text{erf} \left( \frac{v_{\min} + v_{\oplus}}{v_0} \right) - \text{erf} \left( \frac{v_{\min} - v_{\oplus}}{v_0} \right) \right], \quad (11)$$

we obtain from Eqs. (4) and (5)

$$\frac{dR}{dE_R} = \frac{\sigma_{\text{scalar}} \rho_{\chi}}{4v_{\oplus} m_{B^1} m_{\text{red}}^2} F^2(E_R) \left[ \text{erf} \left( \frac{v_{\min} + v_{\oplus}}{v_0} \right) - \text{erf} \left( \frac{v_{\min} - v_{\oplus}}{v_0} \right) \right]. \quad (12)$$

In the above, the value of the local dark matter density  $\rho_{\chi}$  is taken to be  $0.3 \text{ GeV/cm}^3$ . The above expression for the differential rate is for a monoatomic detector like Ge but it can be easily extended for a diatomic detector like NaI as we will see later.

In the present case, the lightest KK state or LKP,  $B^1$ , in the simplest UED is considered to be the candidate for WIMP dark matter [7]. The spin-independent cross section for scattering of  $B^1$  with mass  $m_{B^1}$  off nucleon or nucleus is given by [7]

$$\sigma_{\text{scalar}} = \frac{m_N^2}{4\pi(m_{B^1} + m_N)^2} [Zf_p + (A-Z)f_n]^2,$$

$$f_p = \sum_{\text{all } q} \frac{\beta_q + \gamma_q}{m_q} m_p f_{T_q}^p,$$

$$f_n = \sum_{\text{all } q} \frac{\beta_q + \gamma_q}{m_q} m_n f_{T_q}^n,$$

$$\beta_q = m_q \frac{e^2}{\cos^2 \theta_W} \left[ Y_{qL}^2 \frac{m_{B^1}^2 + m_{q_L}^2}{(m_{q_L}^2 - m_{B^1}^2)^2} + (\text{L} \rightarrow \text{R}) \right],$$

$$\gamma_q = m_q \frac{e^2}{2 \cos^2 \theta_W} \frac{1}{m_h^2}. \quad (13)$$

In Eq. (13),  $m_N$  is the nuclear or nucleon mass,  $q$  denotes the quarks,  $Y$  is the hypercharge and  $m_h$  is Higgs mass. For the KK quark mass  $m_{q^1}$  we follow Ref. [7] and define a degeneracy parameter  $d = (m_{q^1} - m_{B^1})/m_{B^1}$  and then assign different values of  $d$  for the actual calculation of LKP dark matter detection rates.<sup>2</sup> Thus we have three parameters in the calculations, namely  $m_{B^1}$ , the mass of LKP dark matter, the degeneracy parameter  $d$  (or KK quark mass  $m_{q^1}$ ), and the Higgs mass  $m_h$ .

The measured response of the detector by the scattering of WIMP off detector nucleus is in fact a fraction of the actual recoil energy. Thus the actual recoil energy  $E_R$  is quenched by a factor  $qn_X$  (different for different nucleus  $X$ ) and we should express differential rate in Eq. (12) in terms of  $E = qn_X E_R$ . For the Ge detector the expected energy spectrum per energy bin can be expressed as

$$\frac{\Delta R}{\Delta E}(E) = \int_{E/qn_{\text{Ge}}}^{(E+\Delta E)/qn_{\text{Ge}}} \frac{dR_{\text{Ge}}}{dE_R}(E_R) \frac{dE_R}{\Delta E} \quad (14)$$

and for a diatomic detector NaI, the above expression takes the form

$$\begin{aligned} \frac{\Delta R}{\Delta E}(E) = & a_{\text{Na}} \int_{E/qn_{\text{Na}}}^{(E+\Delta E)/qn_{\text{Na}}} \frac{dR_{\text{Na}}}{dE_R}(E_R) \frac{dE_R}{\Delta E} \\ & + a_{\text{I}} \int_{E/qn_{\text{I}}}^{(E+\Delta E)/qn_{\text{I}}} \frac{dR_{\text{I}}}{dE_R}(E_R) \frac{dE_R}{\Delta E}, \end{aligned} \quad (15)$$

where  $a_{\text{Na}}$  and  $a_{\text{I}}$  are the mass fractions of Na and I, respectively, in a NaI detector and are given by (see Table I)

$$a_{\text{Na}} = \frac{m_{\text{Na}}}{m_{\text{Na}} + m_{\text{I}}} = 0.153, \quad a_{\text{I}} = \frac{m_{\text{I}}}{m_{\text{Na}} + m_{\text{I}}} = 0.847.$$

In this work, theoretical prediction of the differential rate is calculated with  $\Delta E = 1 \text{ keV}$ .

<sup>2</sup>The same technique is adopted for  $m_{q^1}$  in Ref. [22].

TABLE I. Mass excess  $\Delta$  (in MeV) and calculated nuclear mass  $m_{\text{nuc}}$  for three nuclei used for WIMP detection.

Nucleus	$\Delta$ (MeV)	Ref.	$m_{\text{nuc}}$ (GeV)
$^{76}_{32}\text{Ge}$	-73.2127	[28]	71.2757
$^{23}_{11}\text{Na}$	-9.5295	[28]	21.5805
$^{127}_{53}\text{I}$	-88.988	[28]	119.1397
$^{131}_{84}\text{Xe}$	-88.415	[28]	122.8985

### III. CALCULATION OF WIMP DETECTION RATES FOR GERMANIUM, NaI, AND XENON DETECTORS

In order to calculate the theoretical predictions for the variation of detected signals with  $E$ , we use Eqs. (12)–(15) along with Eqs. (3),(6)–(9). The scalar cross section for scattering of LKP dark matter off detector nucleus is estimated using Eq. (13). For  $f_{T_q}^x$  ( $x=p$  or  $n$ ), we adopt the central values of these quantities given in [7]. Thus,  $f_{T_u}^p=0.020$ ,  $f_{T_d}^p=0.026$ ,  $f_{T_s}^p=0.118$ ,  $f_{T_u}^n=0.014$ ,  $f_{T_d}^n=0.036$ ,  $f_{T_s}^n=0.118$ , and  $f_{T_{c,b,t}}^x=2(1-f_{T_u}^x-f_{T_d}^x-f_{T_s}^x)/27$ .

The WIMP-nucleus scalar scattering cross sections are evaluated by replacing  $m_N$  in Eq. (13) by mass of the nucleus  $m_{\text{nuc}}$  and using the values of  $f_p$  and  $f_n$  as given above. The nuclear mass  $m_{\text{nuc}}$  is calculated using the relation  $m_{\text{nuc}}=[Zm_p+(A-Z)m_n]+\Delta-Zm_e$ , where  $m_p$  and  $m_n$  are, respectively, the mass of the proton and neutron and  $m_e$  is the mass of electron ( $=0.511$  MeV). The mass excess is denoted as  $\Delta$ . Table I gives the values of  $\Delta$  (in MeV) and calculated values of  $m_{\text{nuc}}$  for  $^{76}_{32}\text{Ge}$ ,  $^{23}_{11}\text{Na}$ ,  $^{127}_{53}\text{I}$ , and  $^{131}_{84}\text{Xe}$  nuclei.

The differential detection rates are computed using Eqs. (4)–(15). As mentioned earlier we have chosen the LKP mass range such that  $600 \text{ GeV} \leq m_{B1} \leq 1200 \text{ GeV}$ . The Higgs mass  $m_h$  is taken as  $120 \text{ GeV}$ . The choice of the third parameter  $d$  is discussed later.

We first calculate differential rates  $dR/dE_R$  [Eq. (12)] for a wide range of values of recoil energy  $E_R$  with  $v_0 = 220 \text{ km/s}$ . The value of  $t$  in Eq. (8) is fixed at  $t_0$ , i.e., the calculations are for June 2. Then we use Eqs. (14),(15) for predicting the observable rate  $\Delta R/\Delta E$  in the units of  $\text{kg}^{-1} \text{ day}^{-1} \text{ keV}^{-1}$ . The quenching factor for Ge is  $qn_{^{76}\text{Ge}}=0.25$  [19], and for  $^{23}\text{Na}$ ,  $^{127}\text{I}$ ,  $^{131}\text{Xe}$  it is  $qn_{^{23}\text{Na}}=0.30$  [21],  $qn_{^{127}\text{I}}=0.09$  [21], and  $qn_{^{131}\text{Xe}}=0.80$  [19], respectively. The value of  $\Delta E=1 \text{ keV}$  ( $E=qn_X E_R$ ).

For the actual calculation we first estimate the range of recoil energy  $E$  for each detector material up to which the calculation is significant. This can be found out by determining at what recoil energy  $E_R$  the differential rate falls down considerably. To this end we write Eq. (12) as

$$\frac{dR}{dE_R} = T_1 T_2 T_3, \quad (16)$$

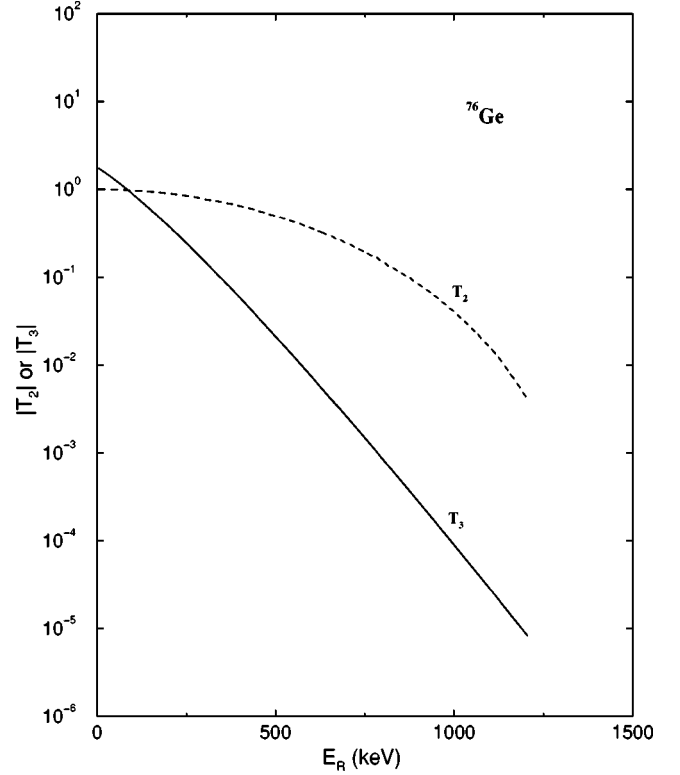


FIG. 1. Variation of  $|T_2|$  and  $|T_3|$  with recoil energy  $E_R$  [see text and Eqs. (12) and (17)] for  $^{76}\text{Ge}$ .

where

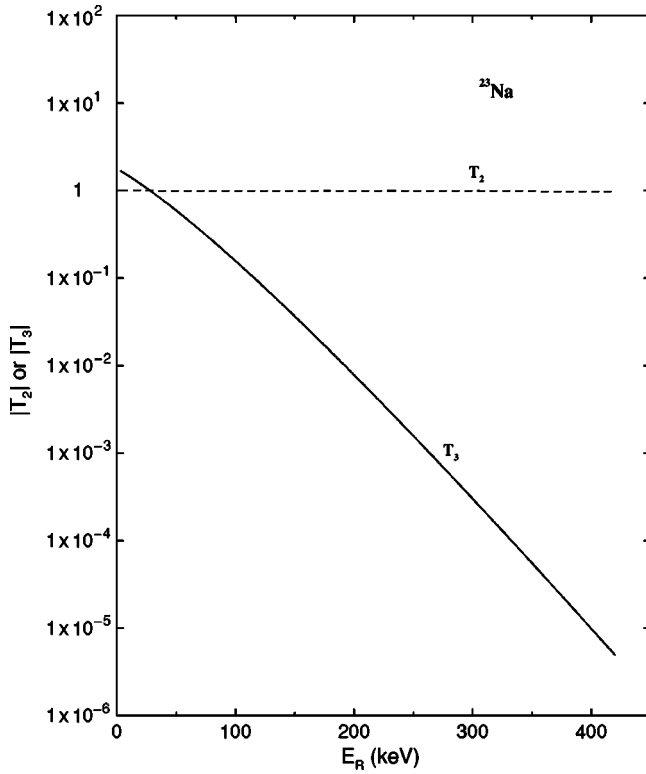
$$T_1 = \frac{\sigma_{\text{scalar}} \rho_X}{4v_{\oplus} m_{B1} m_{\text{red}}^2},$$

$$T_2 = F^2(E_R),$$

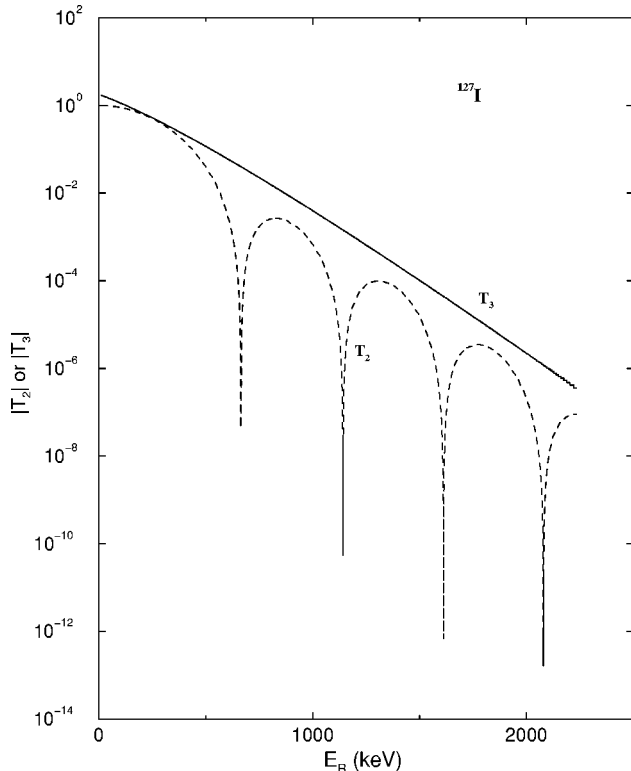
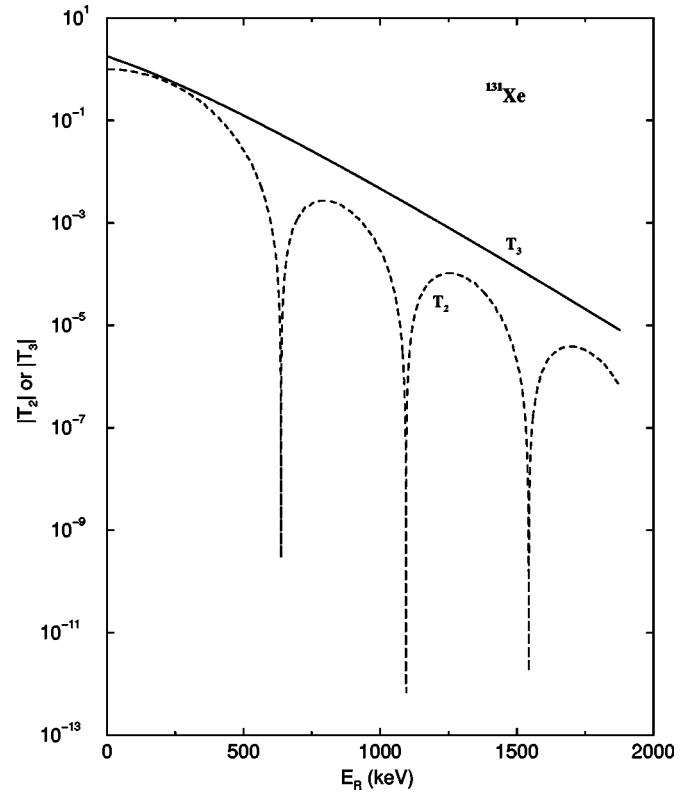
$$T_3 = \left[ \text{erf}\left(\frac{v_{\min} + v_{\oplus}}{v_0}\right) - \text{erf}\left(\frac{v_{\min} - v_{\oplus}}{v_0}\right) \right]. \quad (17)$$

In the above equation the last two terms  $T_2$  and  $T_3$  are dependent on  $E_R$  and hence we should look for the behavior of these terms to estimate the range of  $E_R$  (and hence  $E$ ) up to which the rates are to be calculated. To this end we calculate in Figs. 1–4 the variation of magnitudes,  $|T_2|$  and  $|T_3|$  with  $E_R$  for the case of the detector materials considered here. We take the cutoff value for  $|T_3|$  to be  $10^{-5}$ . We have also checked that the value of  $T_1$ , for all the three detector materials and the mass range ( $m_{B1}$ ) considered, never exceeds  $\sim 2 \times 10^{-8}$ . The corresponding value of  $E_R$  will then give the estimate of the range for the recoil energy  $E_R$ . The range for recoil energy  $E$  actually experienced by the detector can then be estimated using the relation  $E=qn_X E_R$ ,  $qn_X$  being the quenching factor as mentioned earlier. Moreover, as these two terms  $T_2$  and  $T_3$  give the variations of rates with  $E$  (or  $E_R$ ), these plots (Figs. 1–4) will help us understand the nature (shape) of variations of differential rate with observed recoil energy  $E$ . We will see shortly that the factor  $T_2$  greatly influences the shape of  $\Delta R/\Delta E$  vs  $E$  plots.



FIG. 2. Same as Fig. 1 but for  $^{23}\text{Na}$ .

In Fig. 1 we plot the variation of  $|T_2|$  and  $|T_3|$  with  $E_R$  for a  $^{76}\text{Ge}$  detector material. As seen from the plot, the value of  $|T_3|$  falls to the value  $\sim 10^{-5}$  (our cutoff value for  $|T_3|$ ) for

FIG. 3. Same as Fig. 1 but for  $^{127}\text{I}$ .FIG. 4. Same as Fig. 1 but for  $^{131}\text{Xe}$ .

$E_R \sim 1.2$  keV. With  $qn_{^{76}\text{Ge}} = 0.25$ , we estimate the range for recoil energy  $E$  for  $^{76}\text{Ge}$  in the present calculation as  $E = 0.25 \times 1200 = 300$  keV. The variation (shape) of  $T_2$  is mainly governed by the Bessel function which appeared in Eq. (6).

For the case of NaI, we observe the variation of  $|T_2|$  and  $|T_3|$  with  $E_R$  separately for  $^{23}\text{Na}$  and  $^{127}\text{I}$ . The larger estimate for the range of  $E$  between these two is to be taken as the range of  $E$  for NaI. From Fig. 2, the estimated range for  $E$  for the case of  $^{23}\text{Na}$  is taken as (with  $qn_{^{23}\text{Na}} = 0.30$ )  $E = 0.30 \times 400 = 120$  keV.

The influence of the Bessel function for the variation of  $|T_2|$  is evident in Fig. 3 where  $|T_2|$  and  $|T_3|$  are plotted against  $E_R$  for the case of  $^{127}\text{I}$ . From Fig. 3 we estimate the range for  $E$  to be  $E \approx 0.09 \times 1700 \approx 150$  keV ( $qn_{^{127}\text{I}} = 0.09$ ). Thus the estimate of range of recoil energy  $E$  for calculation of differential rate for the case of NaI detector material is 150 keV.

From similar plots in Fig. 4 for  $^{131}\text{Xe}$  detector material, although the estimated range for  $E$  is  $E = 0.80 \times 1800 = 1440$  keV, we have checked that it is enough to consider the range to be up to 450 keV. We have also checked that for annual rate calculations for  $^{131}\text{Xe}$  (Fig. 11) where the differential rate is to be integrated over a day, the results remain unchanged even if we go beyond 450 keV.

The degeneracy parameter  $d$ , as mentioned earlier, is introduced for the KK quark mass  $m_{q^1}$ . Although the masses of  $q^1$  and  $B^1$  may be almost degenerate [7], in order to estimate how the differential detection rate changes for different values of  $d$ , we have considered an example of  $^{76}\text{Ge}$  detector

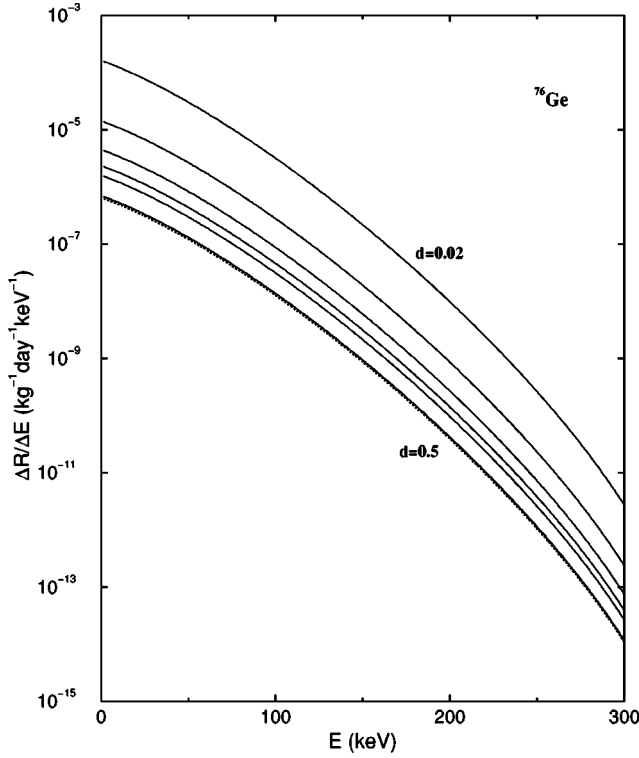


FIG. 5. Differential detection rate  $\Delta R/\Delta E$  vs recoil energy  $E$  for seven different values of degeneracy parameter  $d$ , namely, 0.02, 0.04, 0.06, 0.08, 0.1, 0.3, and 0.5. The topmost plot corresponds to  $d=0.02$  and the lowermost plot corresponds to  $d=0.5$ . The plots in between are for the other values of  $d$ , respectively, given above.

with  $m_{B^1}=800$  GeV. In Fig. 5 we show the calculation of differential rates ( $\text{kg}^{-1} \text{day}^{-1} \text{keV}^{-1}$ ) for seven different values of  $d$ . These values for  $d$  are 0.02, 0.04, 0.06, 0.08, 0.1, 0.3, and 0.5. The uppermost plot in Fig. 5 is for  $d=0.02$  while the lowermost plot corresponds to  $d=0.5$ . The plots in between are for the other five values of  $d$  given above with increasing order of magnitude. In the present calculation of differential detection rates for  $^{76}\text{Ge}$ , NaI, and  $^{131}\text{Xe}$  detectors, however, we have taken the value of  $d$  to be 0.03.

The differential detection rates  $\Delta R/\Delta E$  ( $\text{kg}/\text{day}/\text{keV}$ ) for different values of observed recoil energy  $E$  are calculated using Eqs. (1)–(15) for three types of detector materials, namely,  $^{76}\text{Ge}$ , NaI, and  $^{131}\text{Xe}$ . These calculations are performed for three values of  $m_{B^1}$ , namely, 600, 900, and 1200 GeV. The results are shown in Figs. 6–8, respectively, for the three types of detectors. In Figs. 6–8 we have one feature in common. The differential detection rate decreases as the mass of  $B^1$  increases. This feature is mainly due to  $1/(m_B m_{\text{red}}^2)$  behavior of the rate equation [Eqs. (12,16,17)] and also due to a decrease of  $\sigma_{\text{scalar}}$  with  $m_{B^1}$  in the factor  $T_1$  of the rate equation. The kink that appears in Fig. 7 for the case of the NaI detector can now be easily explained from Figs. 2 and 3. This is mainly due to the behavior of the Bessel function appearing in Eq. (6). Had the energy range been increased further for the case of  $^{76}\text{Ge}$  and  $^{131}\text{Xe}$  detectors, similar kinks would have been observed in Figs. 5, 6, and 8 too but then the signal would be insignificant. From these observations, it can be said that the nuclear form

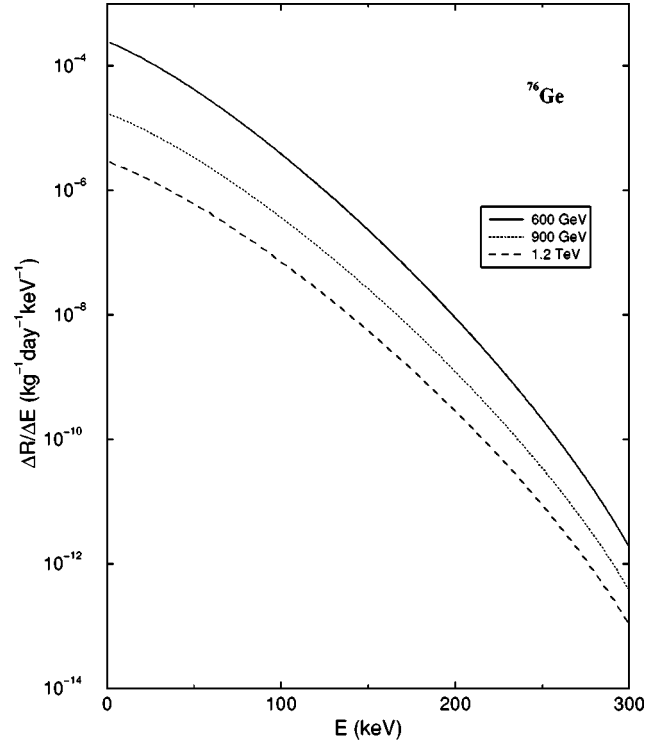


FIG. 6. Differential detection rates  $\Delta R/\Delta E$  ( $\text{kg}/\text{day}/\text{keV}$ ) vs the actual recoil energy  $E$  (keV) for  $^{76}\text{Ge}$  for three different values of  $m_{B^1}$ , namely, 600 GeV, 900 GeV, and 1.2 TeV. The value of  $d$  is fixed at 0.03.

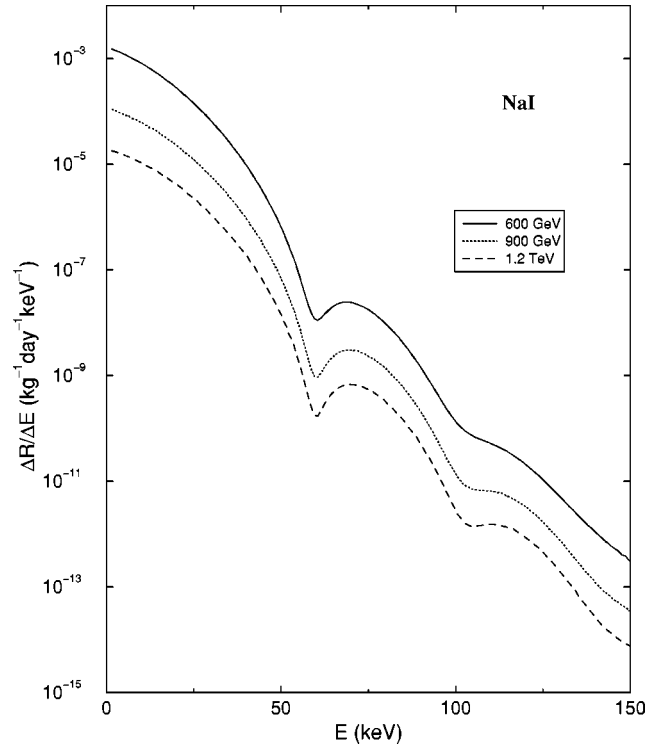
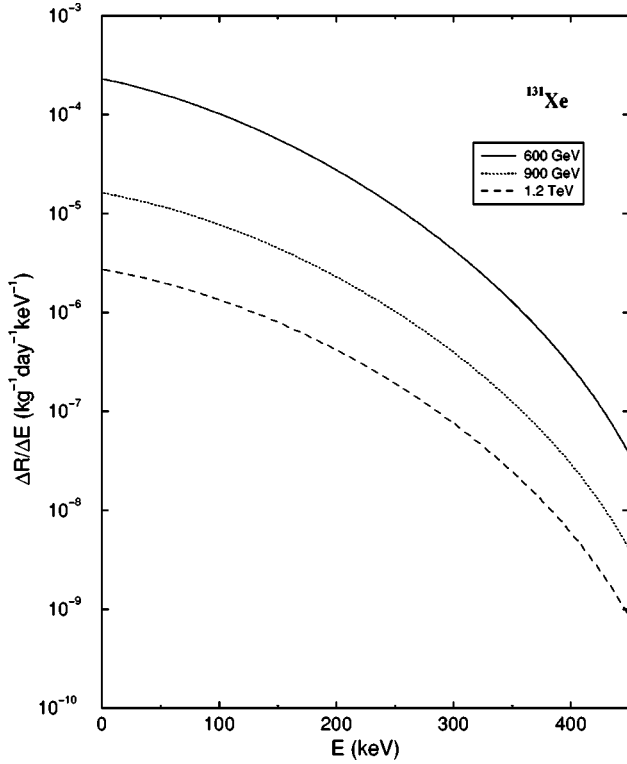
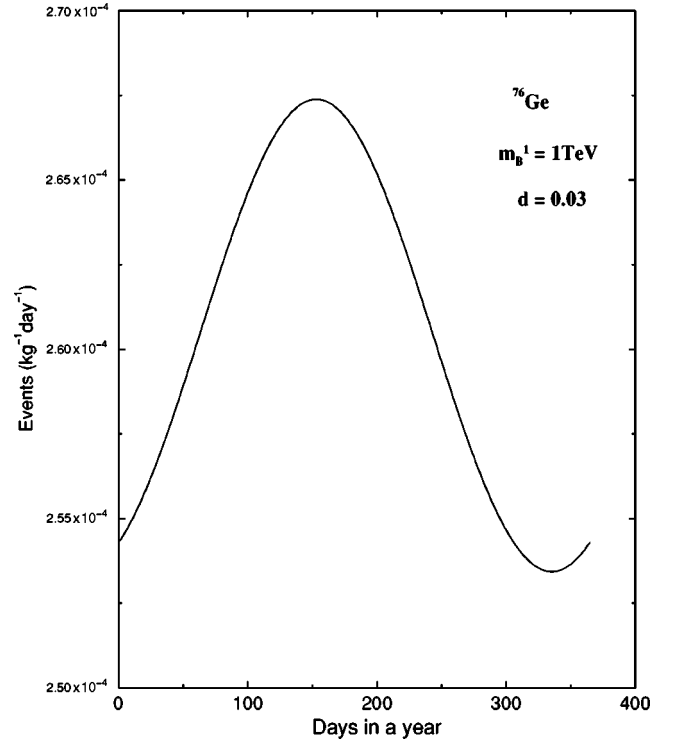


FIG. 7. Same as Fig. 6 but for NaI.

FIG. 8. Same as Fig. 7 but for  $^{131}\text{Xe}$ .

factor plays an important role in the direct detection rates for dark matter. As nuclear form factor depends on nuclear potential, it is also important to properly evaluate this quantity. For the present calculation we have taken the standard expression for nuclear form factor given in [23,24,25].

To this end, it may be mentioned that in a recent work by Servant *et al.* [22], the results for such direct detection rate calculations for LKP dark matter are furnished for three types of detector materials, namely,  $^{73}\text{Ge}$ , NaI, and  $^{131}\text{Xe}$ . But they have given the variation of  $dR/dE_R$  with  $E_R$  with  $m_{B^1}=1\text{ TeV}$  instead of  $\Delta R/\Delta E$  against  $E$  ( $E = \text{quenching factor} \times E_R$ ) as is given in this paper. In the present work this is obtained (for  $m_{B^1}=600\text{ GeV}$ ,  $900\text{ GeV}$ ,  $1.2\text{ TeV}$ ) by first computing  $dR/dE_R$  and then integrating over the energy interval between  $E_R$  and  $E_R + dE_R$  that corresponds to the interval between  $E$  and  $E + \Delta E$  with  $\Delta E = 1\text{ keV}$  [Eqs. (14),(15)]. From earlier discussions, and from Eqs. (12)–(15), it is evident that the differential detection rate has a complicated dependence on many parameters like degeneracy parameter  $d$ ,  $f_p$ ,  $f_n$  [Eq. (13)], the mass of LKP dark matter  $m_{B^1}$ , the velocity of the solar system  $v_\odot$  and hence  $v_\oplus$ , nuclear form factor, etc. Changes in any of these parameters can affect significantly the calculated detection rates. The dependence of rate on  $d$  is demonstrated in Fig. 5 for a  $^{76}\text{Ge}$  detector. In the present work the value of degeneracy parameter  $d$  is taken to be 0.03 whereas for the results shown in [22],  $d=0.15$ . Also the value  $v_\oplus$  used in this work [see Eqs. (8),(9)] can be different for the work of [22]. All these factors contribute to the difference in results obtained in the present calculations and those in Ref. [22].

FIG. 9. Annual variation of LKP dark matter direct detection signal (events/kg/day vs each day in a year) for a  $^{76}\text{Ge}$  detector with  $m_{B^1}=1.0\text{ TeV}$ .

Due to the Earth's motion around the Sun, the directionality of the Earth's motion changes over the year. This in turn induces an annual variation of the WIMP speed relative to the Earth (maximum when the Earth's rotational velocity adds up to the velocity of the solar system and minimum when these velocities are in opposite directions). This phenomenon imparts an annual variation of WIMP detection rates at terrestrial detectors. Therefore investigation of annual variation of WIMP detection rate is a useful method to confirm the WIMP detection. In order to investigate the annual variation of WIMP detection rates we calculate the variation of total rate in one year. In doing this, we vary  $t$  (the day variable) in Eq. (8) from 1 to 365 and for each value of  $t$  (i.e., for each day from January 1) calculate the total rate by integrating the differential rate over the recoil energy range. For these calculations we take  $m_{B^1}=1\text{ TeV}$  and degeneracy parameter  $d=0.03$ . The results for annual variations of the events (/kg/day) for three types of detectors considered are furnished in Figs. 9–11, respectively. All the plots in Figs. 9–11 show the sinusoidal behavior of WIMP detection rate with respect to different days in a year. The prediction for maximum detection is in June and the minimum is in December, as expected.

Although all the investigations above are for a fixed value of  $v_0=220\text{ km/s}$ , we repeat the calculations for five representative values of  $v_0$  in the range  $170\text{ km/s} \leq v_0 \leq 270\text{ km/s}$ . We calculate the variation of differential rates with  $E$  (in keV) for the five values  $v_0=170, 200, 230, 250$ , and  $270\text{ km/s}$ , with the value of  $t$  in Eq. (8) fixed at  $t_0$  and  $m_{B^1}=700\text{ GeV}$ ,  $d=0.03$ . The results for the  $^{76}\text{Ge}$  detector

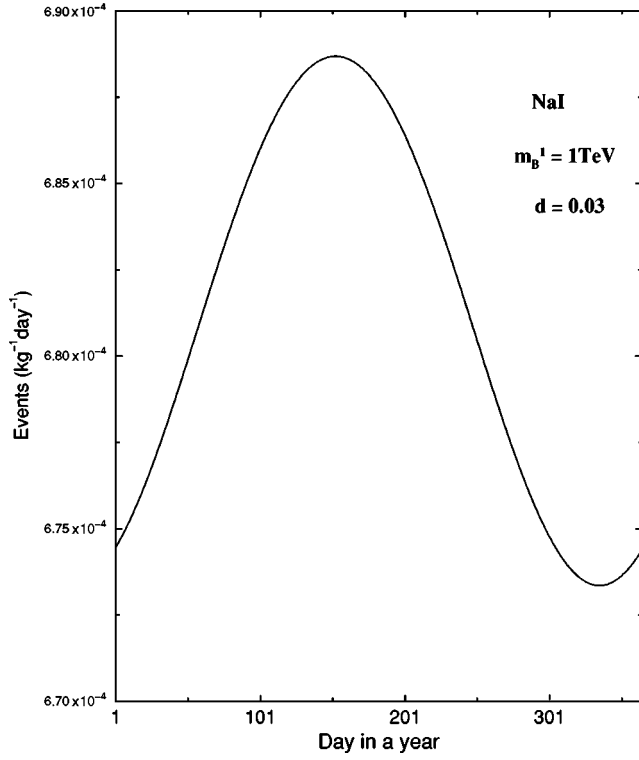
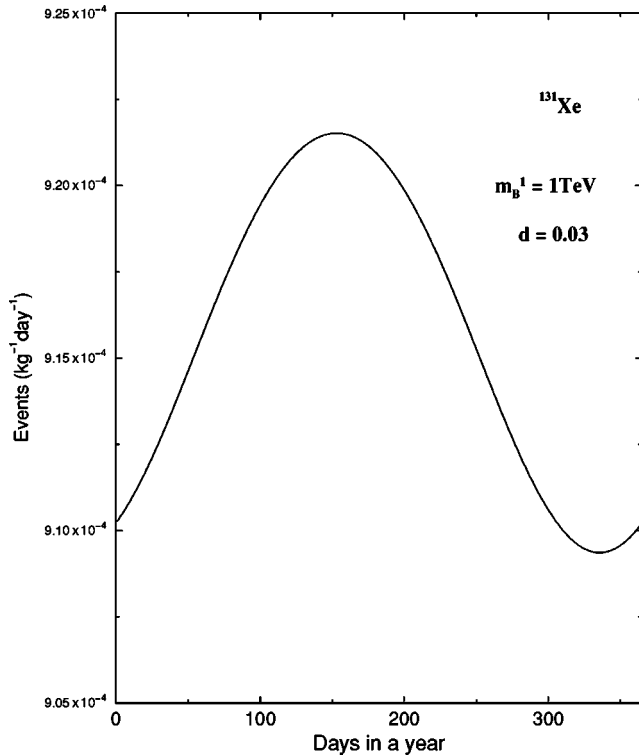
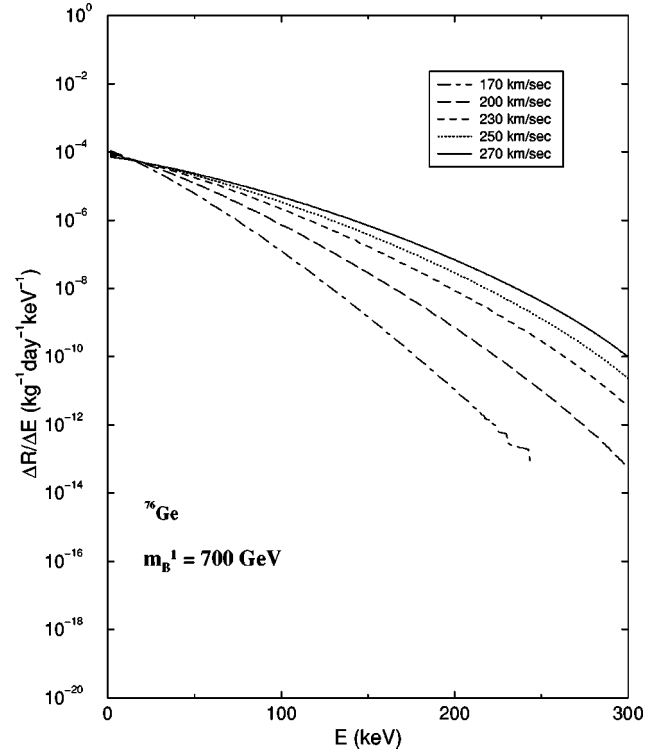


FIG. 10. Same as Fig. 9 but for NaI.

are plotted in Fig. 12 and those for the NaI detector are furnished in Fig. 13. Both Figs. 12 and 13 show that although at low energy the rates corresponding to different values of  $v_0$  are not very different from each other, for higher

FIG. 11. Same as Fig. 10 but for  $^{131}\text{Xe}$ .FIG. 12. Differential detection rates  $\Delta R/\Delta E$  (/kg/day/keV) vs the actual recoil energy  $E$  (keV) for  $^{76}\text{Ge}$  for different values of velocities of the Solar System  $v_0$ .

recoil energies the differential detection rate is higher for higher values of  $v_0$ . Thus the results of future dark matter direct detection experiments with increased sensitivity and

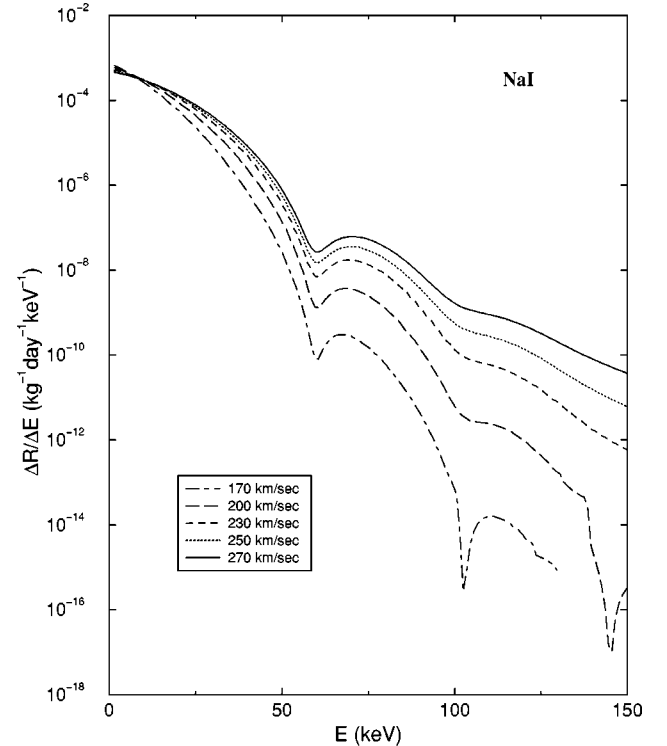


FIG. 13. Same as Fig. 12 but for NaI.



energy range may perhaps be able to determine more precisely the value of the circular velocity of the solar system.

#### IV. DISCUSSIONS AND CONCLUSIONS

We have considered the lowest state Kaluza-Klein particle (LKP) in universal extra dimension to be a candidate for cold dark matter. Unlike the supersymmetric particle, neutralino, which is a fermion, this Kaluza-Klein particle is bosonic. We have calculated differential rates of direct detection of signals in the case of such LKP dark matter for three types of detector materials, namely  $^{76}\text{Ge}$ , NaI, and  $^{131}\text{Xe}$ . Due to the annual motion of the Earth around the Sun, the WIMP signals detected by Earth bound detectors suffer an annual modulation with a maximum when the WIMP velocity with respect to the Earth is parallel to the Earth's rotational velocity and a minimum when they are antiparallel. We have estimated the nature of annual modulation signal for WIMPs for all three types of detectors mentioned above. The annual modulation signature is a characteristic signature in a dark matter direct search experiment. Lastly, we predicted the differential rate for five different values of  $v_0$  within its 90% C.L. range to show the former's variation with the circular velocity of the solar system. The calculations consider three parameters. They are mass of LKP dark matter  $m_{B^1}$ , the degeneracy parameter  $d$  (for KK quark mass  $m_{q^1}$ ), and the Higgs mass  $m_h$ . Estimates can be made for  $m_{B^1}$  from col-

lider bound [10] and from dark matter content in the universe. There are estimates for Higgs mass too but no such estimate is there for the parameter  $d$ . We have seen in Fig. 5 that the detection rate varies  $\sim 10^2$  for the variation of  $d$  from 0.02 to 0.5 for  $^{76}\text{Ge}$ . A more careful estimate for  $d$  is needed.

For the velocity distribution of cold dark matter, we have taken the generally used Maxwellian velocity distribution. This distribution is widely used and is a good approximation. But for future calculations one also should look for a more accurate form of velocity distribution as this quantity is crucial for determining the detection rate and more importantly for the calculation of annual modulation. In a recent work Vegados *et al.* [29] gave a velocity distribution and density profile for CDM, based on Eddington theory. In the present work CDM density  $\rho_\chi$  is taken to be  $0.3 \text{ GeV cm}^{-3}$  which is again the standard practice.

The dark matter direct detection signal can be used as a probe to find the value of  $v_0$  more precisely. The new detectors such as GENIUS, NaI detectors, and the proposed 1000 kg  $^{131}\text{Xe}$  detector along with various other dark matter search programs of increased sensitivity, can verify the possibility of LKP to be a candidate for dark matter.

#### ACKNOWLEDGMENT

The author wishes to thank G. Servant for some valuable suggestions.

- 
- [1] A. Bottino, F. Donato, N. Fornengo, and S. Scopel, Phys. Rev. D **59**, 095003 (1999).
  - [2] A. Bottino, V. de Alfaro, N. Fornengo, G. Mignola, and M. Pignone, Astropart. Phys. **2**, 67 (1994); A. Bottino, F. Donato, N. Fornengo, and S. Scopel, Phys. Rev. D **59**, 095004 (1999).
  - [3] H. Baer and M. Brhlik, Phys. Rev. D **57**, 567 (1998).
  - [4] J. Edsjo and P. Gondolo, Phys. Rev. D **56**, 1879 (1997).
  - [5] U. Chattopadhyay, A. Corsetti, and P. Nath, Phys. Rev. D **66**, 035003 (2002).
  - [6] D. Majumdar, J. Phys. G **28**, 2747 (2002).
  - [7] H.-C. Cheng, J. L. Feng, and K. T. Matchev, Phys. Rev. Lett. **89**, 211301 (2002).
  - [8] H. C. Cheng, hep-ph/0206035.
  - [9] T. Kaluza, Sitzungsber. Preuss. Akad. Wiss. Berlin (Math. Phys.) **K1**, 966 (1921); O. Klein, Z. Phys. **37**, 895 (1926); Surv. High Energy Phys. **5**, 241 (1986).
  - [10] T. Appelquist, H.-C. Cheng, and B. A. Dobrescu, Phys. Rev. D **64**, 035002 (2001).
  - [11] G. Servant and T. M. P. Tait, Nucl. Phys. **B650**, 391 (2003).
  - [12] R. Bernabei *et al.*, Phys. Lett. B **533**, 4 (2000); astro-ph/0205047.
  - [13] CDMS Collaboration D. Abrams *et al.*, Phys. Rev. D **66**, 122003 (2002).
  - [14] EDELWEISS Collaboration, A. Benoit *et al.*, Phys. Lett. B **545**, 43 (2002).
  - [15] H. V. Klapdor-Kleingrothaus *et al.*, Astropart. Phys. **18**, 525 (2003).
  - [16] H. V. Klapdor-Kleingrothaus and B. Majorovits, hep-ph/0103079; H. V. Klapdor-Kleingrothaus, Nucl. Phys. B (Proc. Suppl.) **110**, 364 (2002), and references therein.
  - [17] E. Aprile *et al.*, astro-ph/0207670.
  - [18] T. K. Gaisser, G. Steigman, and S. Tilav, Phys. Rev. D **34**, 2206 (1986).
  - [19] A. Bottino, V. de Alfaro, N. Fornengo, G. Mignola, and S. Scopel, Astropart. Phys. **2**, 77 (1994).
  - [20] P. Belli, R. Bernabei, A. Bottino, F. Donato, N. Fornengo, D. Prosperi, and S. Scopel, Phys. Rev. D **61**, 023512 (2000).
  - [21] M. Brhlik and L. Roszkowski, Phys. Lett. B **464**, 303 (1999).
  - [22] G. Servant and T. M. P. Tait, hep-ph/0209262.
  - [23] G. Jungman, M. Kamionkowski, and K. Griest, Phys. Rep. **267**, 195 (1996).
  - [24] R. H. Helm, Phys. Rev. **104**, 1466 (1956).
  - [25] J. Engel, Phys. Lett. B **264**, 114 (1991).
  - [26] P. J. T. Leonard and S. Tremaine, Astrophys. J. **353**, 486 (1990).
  - [27] C. S. Kochanek, Astrophys. J. **457**, 228 (1996).
  - [28] *Table of Isotopes*, 8th ed., edited by R. B. Firestone and V. S. Shirley (Wiley, New York, 1996), Vol. 1.
  - [29] J. D. Vergados and D. Owen, astro-ph/0203293.